Evaluating the performance of satellite rainfall estimates using data from NAME program

Ismail Yucel
Hampton University, Center for Atmospheric Sciences, Hampton, VA 23668
Ismail.yucel@hamptonu.edu; 757-728 6729, Fax: 757-727 5090
Robert J. Kuligowski
NOAA-NESDIS, Camp Springs MD
David Gochis
NCAR

Abstract

This study investigates the performance of the NESDIS Hydro Estimator (HE) rainfall algorithm against observations taken from the North American Monsoon Experiment (NAME) program. A recent rainfall observation network established in NAME program provides precipitation measurements of convective origin over large complex topographical areas while comprehensive validations of the satellite-estimated precipitation characteristics such as the frequency, intensity, diurnal evaluation and its relation to the complex regional topography have been absent to date due to the unavailability of pre-existing dense observation network. The independence of the HE on radar data, on the other hand, makes its applicability appropriate for mountainous regions. The rainfall estimates are validated against the measurements obtained through Aug 2 to Sep 14, 2002 to report whether the results from the HE is capable of capturing terrain-induced precipitation characteristics. It seems that satellite estimates are able to capture main characteristics of terrain-induced precipitation during this comparison period.

1. Introduction

Visible and infrared (IR) imagery and passive microwave instruments are the satellite tools that have been used extensively to estimate stratiform and convective type of precipitation for a range of applications from climate-scale to instantaneous event. Although the microwave techniques with polar-orbiting sun-synchronous satellites are more physically direct while responding to precipitation-size hydrometeors within clouds rather than cloud-top temperature or albedo, the visible and IR based techniques are widely used in the depiction of the intensity and spatial extent of heavy precipitation due to their high frequency (15 min) and high spatial resolution (~ 4 km) measurements from Geostationary Operational Environmental Satellite (GOES). These satellites with their broad area coverage are therefore more suitable in operational use for estimation of extreme-precipitation events. Vicente et al. (2002) reported that it is possible to accurately observe rapidly developing thunderstorms at very high spatial and temporal resolutions with improved capabilities of the current geostationary satellites.

In support of the National Weather Service's (NWS) flash flood warnings and heavy precipitation forecasts efforts, the National Oceanic and Atmospheric Administration/National Environmental Satellite Data and Information Service (NOAA/NESDIS) Office of Research and Application (ORA) has been providing satellite precipitation estimates operationally since 1978. Operational satellite rainfall estimates are originated with the Interactive Flash Flood Analyzer (IFFA) (Scofield and Oliver 1977 and Scofield 1987) following the technique based on GOES longwave IR window (10.7 μm). To improve timeliness of the IFFA and to extend areal coverage of products, NESDIS developed an automatic algorithm called the Auto-Estimator (AE) (Vicente et al. 1998). In addition to IR window brightness temperature, the AE has the features of environmental moisture, cloud growth, cloud-top structure, orographic and parallax corrections (Vicente et al. 2002), and a convective equilibrium level adjustment for warm-top events (Scofield 2001). As reported by Scofield (2001) and Scofield and Kuligowski (2003), the AE increased its productivity in terms of monitoring a greater number of heavy-rainfall and disseminating a greater number of satellite-precipitation-estimation messages in a more timely fashion. However, despite the use of temperature trends to distinguish cloud-tops between thick convective clouds and thin cirrus clouds in the AE, it still considerably overestimated the areal extent of rainfall reported in Rozumalski (2000) and Scofield and Kuligowski (2003). To overcome this problem, the AE algorithm uses 15-minute Weather Service Radar-1988 Doppler (WSR-99D) reflectivity data. As this addition alleviated the overestimation in spatial extent of rainfall, the dependence of the AE on radar makes its applicability inappropriate for regions with inadequate rainfall information from radar and/or rain gauges. In response to these concerns, NESDIS developed another version of the AE, called the Hydro-Estimator (HE), which is following a different approach for discriminating raining areas from non-raining without usage of radar as well as new adjustments for moisture availability effects. The statistical analysis of Scofield and Kuligowski (2003) showed that both the HE and AE with radar data have the similar performance, making the HE more preferable in operational use. Consequently, over mountainous regions lacking radars and dense networks of rain gauges, the HE algorithm offers operational rainfall data with high spatial and temporal resolution, which is crucial in flash flood forecasting as weather conditions can very greatly over short distances and cause weather-related hazards.

Although large-scale atmospheric motions control the general stability or instability in the atmosphere, local topographic effects are critical to the spatial and temporal distribution of convective activity because of the characteristics of the flow disturbances created by the mountains (Adams and Comrie, 1997 and Vicente et al., 2002). In general, precipitation amounts tend to increase with height as the greater amount of rainfall is located windward of the orographic crest. Vicente et al. (2002) showed that orographic correction of the AE algorithm enhanced precipitation distribution over the US west coast when comparing the results from the AE without correction. In their study, however, a thorough validation of this correction procedure was not carried out due to the lack of dense network of surface rainfall measurements. Furthermore, comprehensive validations of the satellite-estimated precipitation character such as the hourly frequency, intensity, diurnal evaluation and its relation to the complex local topography have been absent to date due to the unavailability of pre-existing dense observation network in mountainous regions. However, as part of the North American Monsoon Experiment (NAME) program, which has been developed to aim at improving both understanding and predictability of warm season precipitation in southwest US, a recent technical note (Gochis et al. 2003b) documented the establishment of a new event-based rain gauge network, known as the NAME Event Rain gauge Network (NERN), in northwest Mexico. Results presented in Gochis et al. (2003b and 2004) demonstrated the ability of the new network to capture high-resolution temporal aspects and general physiographic aspects of North American Monsoon (NAM) precipitation as these features are critical for the validation of remotely sensed and modeled precipitation estimates.

The primary goal of the research in this study was to investigate the HE algorithm's performance in documenting surface precipitation on topographically complex region of NAME and thus to report whether the HE is capable of capturing the aspects of terrain-induced rainfall and to define where algorithm improvement may be required. The 50 gauges of NERN sampled according to the temporal aspects of precipitation with respect to topography were used to compare with the 4-km rainfall estimates of the HE for the period of 2 Aug–14 Sep 2002, this being the period of NAM. It is envisaged that such evaluation will also be helpful to users of mesoscale atmosphere modelers as these models have the severe uncertainty in predicting convective systems at high spatial resolution due to the strong insolation and the presence of elevated heat sources associated with the complex topography over the US southwest (Yucel et al., 2002 and 2003).

2. Description of study area and rainfall algorithm

2.1 Observational arrays

In support of coordinated field activities of the NAME, a new event-based surface rain gauge network was installed in two phases corresponding to the 2002 and 2003. A network of the 50 tipping-bucket rain gauges installed over the month of July and the first days of August 2002 was shown in Fig. 1. The 48 of these total rain gauges providing data for the entire selected comparison period from 2 Aug–14 Sep 2002 was used in this study. As seen from Fig. 1, the network configuration used in this research consists of the 5 west-east transects through the formidable Sierra Madre Occidental (SMO) mountains. The network does not present the most favorable installment for measuring the spatial pattern of convective rainfall while it provides instantaneous precipitation effectively on longitudinal extend with respect to the distribution of terrain elevation. Gochis et al. (2003b and 2004) divided the elevation into six groups to show the rainfall sampling as a function of elevation. The same elevation breakdown is also used in the research here that validates satellite rainfall estimates. A map of the elevation bands overlain with the 50 rain gauges is shown in Fig. 1. The overall range in elevation sampled by the network is between 71 m and 2979 m with the mean value of 1226 m. This sampling possesses a well-matched distribution of rain gauges with respect to elevation to avoid a low-elevation bias with the regional topography. For example, there are 13 gauges located at over 2000-m elevation, which are also critical for analyzing temporal features of terrain-induced convective precipitation. The dearth of the gauges located in the 1000-1500-m (elevation band 3) is because there is comparatively little terrain in this elevation band along the western slope of the SMO as it is apparent from Fig. 1. Gochis et al. (2004) notes that the NERN configuration is adequate for sampling the variability in precipitation frequency and relative intensity as a function of regional topographic gradients while the typical distance between NERN gauges is on the order of several tens of kilometers along a transect and up to hundreds of kilometers between transects.

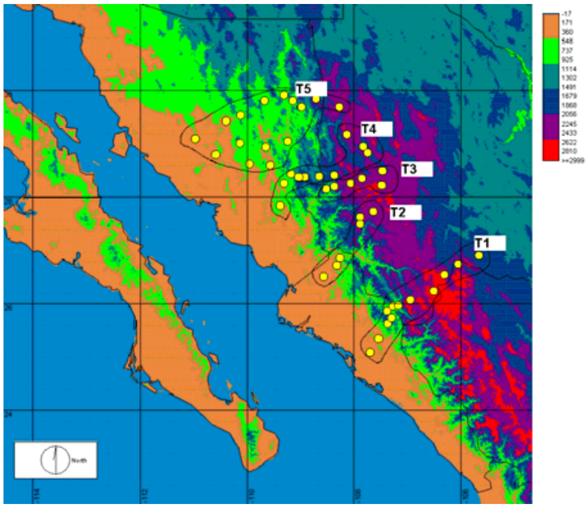

Figure 1: Shows the map of the elevation bands overlain with 50 rain gauges. Each color corresponds to an elevation band.

2.2. Rainfall algorithm

Among several operational algorithms developed for quantitative precipitation estimation (QPE) at NESDIS, the HE from Scofield and Kuligowski (2003) is selected to use in this study because of its timeliness and applicability over mountainous areas. The HE computes real time estimates of instantaneous rain rate using 10.7-µm brightness temperatures based on a curve that was originally derived from 6800 pairs of collocated IR brightness temperatures and radar rainfall rates for the development of the AE algorithm

Unlike the AE algorithm, the HE defines the raining pixels as “convective core” and “non-core” precipitation and assigns a rain rate that is a combination of the two depending on the spatial characteristics of the predetermined region surrounding the pixel of interest. This region can cover an area of interest up to a 50-pixel radius for cloud tops colder than 200 K, or up to 30-pixel radius for cloud tops warmer than 220 K depending on the minimum temperature determined using a 101x101-pixel box centered the interested pixel. The presence or absence of precipitation and the fraction of ‘core” and “non-core” precipitation is determined based on a computed index value, which divides the difference of brightness temperatures between the mean of previously selected region and interested pixel to the mean standard deviation of selected region. The rain rate is set to zero if the pixel is warmer than the average of its surroundings (negative index) with the assumption that such pixels are cirrus or convectively inactive clouds. For positive index values constrained to be 1.5 or less, the “core” fraction is related to the index value and the “non-core” fraction is related to (1.5-index). The standard AE rain-rate curve is adjusted according to the difference between the pixel brightness temperature and the average value in the surrounding region. This approach has substantially reduced the exaggeration of rain area exhibited by the AE reported by Scofield and Kuligowski (2003).

A combined factor of precipitable water (PW) and relative humidity (RH) developed to adjust the tendency of precipitation overestimation in the AE (Vicente et al. 1998) was separated, with the PW value used to adjust the rain-rate curve based on moisture availability and the RH value used to derive an amount to be subtracted from the rain rate in the HE. The PW and RH are based on data from the Eta Model. These adjustments improved the handling of stratiform events with embedded convection, and also of wintertime precipitation, which is typically associated with low PW values (Scofield and Kuligowski, 2003). Other adjustment parameters incorporated in the HE are the convective equilibrium (Scofield 2001), the orography and parallax corrections (Vicente et al. 2002), and correction for satellite zenith angle.

3. Results

3.1 Spatial patterns

Horizontal images of total rainfall for observations and satellite from 2 Aug–14 Sep 2002 are shown in Figure 2a and b, respectively. Observed values were generated by interpolating the station values to a grid using a linear interpolation algorithm. The maximum observed precipitation lies along the western slope of the SMO. The core region of maximum precipitation would exist as a more or less continuous band along the western slope according to the NERN configuration. These features are more or less followed by the satellite estimates with a tendency of overestimation over the lower elevation areas. Conversely, satellite retrievals significantly underestimate precipitation over high terrain areas as seen at southeastern part of the map.

3.2 Diurnal cycles

Figure 3 shows the diurnal cycle of hourly precipitation frequency for each of the 5 elevation bands along with the network-mean diurnal cycle. It is evident that precipitation initiates first and most frequently over the high terrain of the SMO. Precipitation frequency in elevation bands 5 and 6 increases beginning around 1200 local solar time following the diurnal minimum in frequency. Below bands 5 and 6, precipitation tends to occur later in the day and into the evening. The latest elevation bands to peak are the lowest elevation bands, 1 and 2. However, the highest elevation bands (5 and 6) represent the lowest frequency in satellite estimates even though they have the earliest peaks as in the observations. Bands 1 and 2 in satellite estimates also show the latest peak in frequency. However, all the bands reach their peak earlier than observations. Figure 4 shows the diurnal cycles of hourly mean precipitation intensity. They display increased hour to hour variability relative to the cycles of precipitation frequency. Both observation and satellite values show that intensity at the highest elevations is comparatively light and less than the network mean intensity.

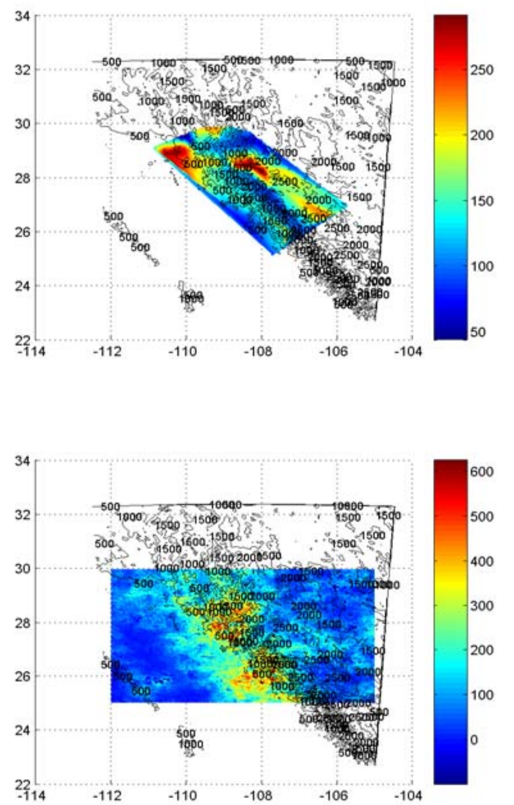

Figure 2: Total rainfall patters over the study site. Contour of topography is also provided at the background. Rain is in mm.

4. Discussions

NOAA-NESDIS rainfall estimates could play a critical role in replacing the poor rainfall estimates from mesoscale atmosphere models. Outcomes of this research will help us to determine future research directions, such as assimilation of satellite precipitation estimates into the mesoscale atmosphere model for making better predictions. We also plan to use these rainfall estimates in hydrological applications associated with flood risk analysis from extreme weather events.

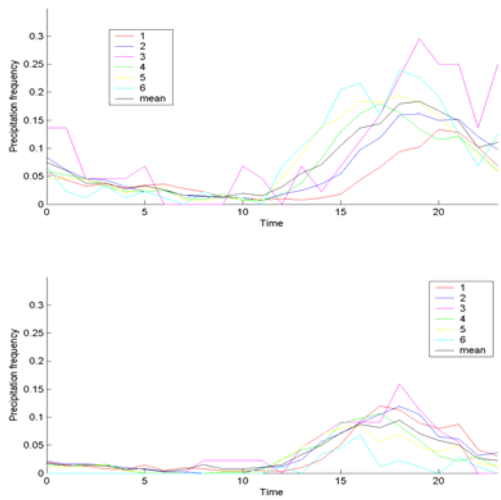

Figure 3: Diurnal cycles of precipitation frequency for each band (a) for observations and (b) for satellite estimates.

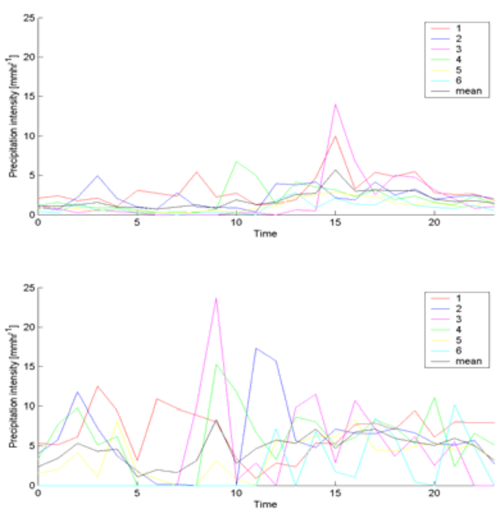

Figure 4: Diurnal cycles of precipitation intensity for each band (a) for observations and (b) for satellite estimates.

5. References

Gochis, D.G., J.-C. Leal, W. J. Shuttleworth, C. Watts, and J. Garatuza-Payan, 2003: Preliminary Diagnostics from a New Event-Based Precipitation Monitoring System in Support of NAME, J. Hydrometeorology, 4, 974-981.

Gochis, D.G., A. Jimenez, C. J. Watts, J. Garatuza-Payan, W. J. Shuttleworth, 2004: Analysis of 2002 and 2003 Warm Season Precipitation from the North American Monsoon Experiment (NAME) Event Rain gauge Network (NERN), Monthly Weather Review, (in press).

Scofield, R. A. and R. J. Kuligowski, 2003: Status and Outlook of Operational Satellite Precipitation algorithms for Extreme-Precipitation Events, Weather and Forecasting, 18, 1037-1051.

Vicente, G. A., J. C. Davenport, and R. A. Scofield, 2002: The role of orographic and parallax corrections on real time high resolution satellite rainfall rate distribution, Int. J. Remote Sensing, 23, 221-230.

Vicente, G. A, R. A. Scofield, and W. P. Menzel, 1998: The operational GOES Infrared Rainfall Estimation Technique, 79, 1883-1898.

Yucel, I., W. J. Shuttleworth, X. Gao, and S. Sorooshian, 2003: Short-Term Performance of MM5 with Cloud-Cover Assimilation from Satellite Observations, Monthly Weather Review, 131, 1797-1810.

Yucel, I., W.J. Shuttleworth, R. T. Pinker, L. Lu, and S. Sorooshian, 2002: Impact of Ingesting Satellite-Derived Cloud Cover into the Regional Atmospheric Modeling System, Monthly Weather Review, 130, 610-628.